NASA

Technical Memorandum 79698

Propulsion-Free Separation and Rendezvous of Small Shuttle Free-Flyers Using Controlled Differential Drag

Joseph C. King

JANUARY 1979

National Aeronautics and
Space Administration

Goddard Space Flight Center
Greenbelt, Maryland 20771

Page intentionally left blank

PROPULSION-FREE SEPARATION AND RENDEZVOUS OF SMALL SHUTTLE FREE-FLYERS USING CONTROLLED DIFFERENTIAL DRAG

Joseph C. King
NASA/Goddard Space Flight Center
Greenbelt, MD 20771

January 1979

To be presented at the AIAA Fifth Sounding Rocket Technology Conference, March 7-9, 1979, Houston, TX. (Paper No. 79-0494)

GODDARD SPACE FLIGHT CENTER
Greenbelt, Maryland

Page intentionally left blank

CONTENTS

ILLUSTRATIONS

ILLUSTRATIONS (Continued)

TABLE

PROPULSION-FREE SEPARATION AND RENDEZVOUS OF SMALL SHUTTLE FREE-FLYERS USING CONTROLLED DIFFERENTIAL DRAG

Joseph C. King*
Goddard Space Flight Center
Greenbelt, Maryland

Abstract

A natural successor in the Shuttle era to many sounding rocket flights is the free-flyer mode of operation, in which the Shuttle Orbiter releases a subsatellite (with payload), effects a desired separation, and finally approaches and retrieves the free-flyer. This paper proposes replacing, to the maximum extent feasible, the propulsive maneuvers required of the Orbiter by equivalent relative motions obtained through controlled differential drag (via changes in free-flyer effective area and/or Orbiter attitude changes). Simplified analytical techniques are developed and feasibility is verified. Several illustrative examples are specified (e.g., a 3-km separation in 1 day, with 4-day return).

Nomenclature

A	frontal (characteristic) area
B	ballistic coefficient, $m/C_D A$, in kg/m^2 (adopted SI units)
BN	ballistic coefficient, $m/C_D A$, in lb/ft^2 (Ref. 1)
C_D	drag coefficient
d	diameter
E	orbital energy
F	force
h	orbital altitude
K	earth gravitational parameter ($GM_\oplus$)
r	radial distance
s	displacement along orbit
S	total displacement
t	time variable
T	orbital kinetic energy
v	velocity
V	orbital potential energy
W	work
x, y, z	Orbiter body axes (Figure 4)
$\hat{x}$, $\hat{y}$, $\hat{z}$, $\hat{v}$	unit vectors in directions of x, y, z, and v
ρ	density
θ	angular displacement
τ	orbital period

Subscripts

a	atmospheric
o	initial
O	Orbiter
ff	free-flyer
rel	relative

Background

A major current concern to many experimenters and others involved in space flight operations is the prospect of sharply increased lead times, costs, and interface complexity involved in the transition to Shuttle-based flight modes. Such a prospect is especially problematical to those whose support and operating arrangements are adapted to the relatively simple and inexpensive procedures routinely followed in sounding rocket flights. Hence any available means for appreciably simplifying the implementation of such Shuttle-based flights are not only intrinsically desirable, but may be crucial to the viability of some valuable applications.

This paper proposes an approach to the needed simplification which is aimed at minimizing the impact on an overall Shuttle mission plan caused by the incorporation of a modest additional payload, to be carried on a free-flying subsatellite.

Basic Proposal

A natural successor in the Shuttle era to many sounding rocket flights is the free-flyer mode of operation, in which the Shuttle Orbiter releases a free-flying subsatellite containing the payload. The free-flyer gradually moves away from the Orbiter and operates independently for an extended period of time, after which the Orbiter retrieves the free-flyer through a series of rendezvous, approach, and capture maneuvers.

During the free flight of the subsatellite, the relative motion between it and the Orbiter is influenced by atmospheric drag, since in general the two bodies will have different ballistic coefficients. Furthermore, such drag-induced relative motion can be harnessed to produce desired maneuvers, provided the drag properties of the two bodies are favorable or can be controlled. Useful drag control of this type proves in fact to be feasible for free-flyer-Orbiter maneuvers, which leads to the simplifying procedure proposed in this paper. It consists of replacing, to the maximum extent feasible, the propulsive maneuvers required of the Orbiter in the separation-rendezvous operation by equivalent relation motions obtained through controlled differential drag. The basic drag maneuvering technique can be applied in several ways and with many variations. For the present purpose of basic feasibility illustration, however, a single relatively simple plan is chosen for discussion and development.

A Specific Scheme

In order to execute both the separation and rendezvous phases of the maneuver sequence using drag alone, it is necessary to reverse the relative motion of the

*Aerospace Engineer, Sounding Rocket Division
Member, AIAA

bodies between the two phases by altering the ballistic coefficient of one or both bodies. To minimize the impact on the Orbiter operating plan, the required modification is confined in this scheme to the free-flyer. This modification is represented schematically in Figure 1 by the release of a balloon which had been attached to the free-flyer during the separation phase to increase its drag. The drag balloon is invoked here for simplified schematic illustration only -- in a working design, a more firmly attached drag device might be chosen instead.

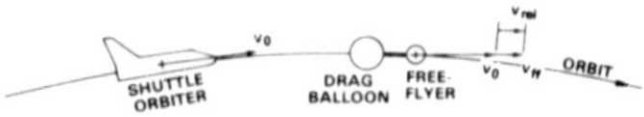

SEPARATION PHASE

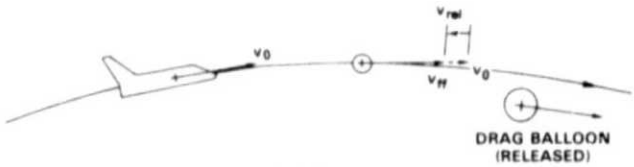

RENDEZVOUS PHASE

Fig. 1 Free-Flyer Separation and Rendezvous Using Detachable Drag Balloon to Reverse Relative Velocity (v_{rel})

Figure 1 depicts the two basic phases of relative motion in the overall operation -- separation (increasing distance between free-flyer and Orbiter) and rendezvous (decreasing distance). During separation, the free-flyer moves ahead of (and a lesser distance below) the Orbiter as a result of the free-flyer's higher drag, induced by the attached balloon. To initiate the rendezvous phase, the balloon is released, resulting in a smaller (relative to the Orbiter) drag acceleration for the free-flyer and a relative forward (and downward) motion of the Orbiter. This relative motion effectively reverses the separation produced in the previous phase. Thus by these simple and essentially passive procedures, the principal maneuvers involved in separation and rendezvous can be accomplished independently of the Orbiter and without propulsion.

For simplicity, only the tangential (along-the-orbit) motions between the two bodies is shown in Figure 1. The radial (downward) motion is substantially smaller, amounting to about 21% of the tangential motion. Addition of the radial component makes the total relative displacement about 2% greater than the tangential displacement alone, as illustrated in Figure 2. For the small displacements considered here, the straight-line, rectangular approximation shown is adequate. The actual relative motion is described in greater detail and approximated analytically in the Appendix.

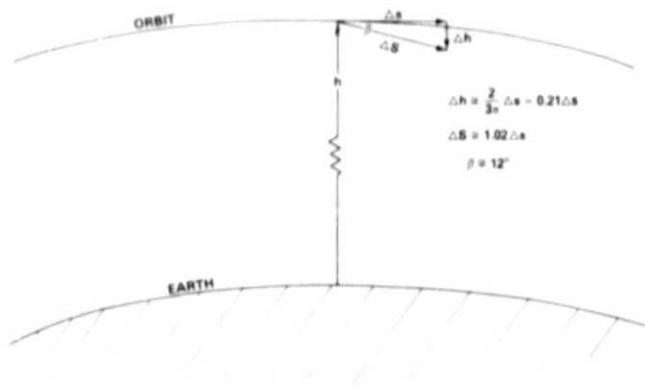

Fig. 2 Motion of Free-Flyer Relative to Orbiter Under Differential Drag for Small Displacements

Feasibility

The basic feasibility of the controlled drag-induced separation and rendezvous proposal hinges on the practicability of achieving Orbiter-free-flyer differential drag accelerations in suitable magnitudes and in both directions. This requirement depends (see Appendix) in turn on the feasibility of achieving suitable values of the ballistic coefficient (B) of the free-flyer, since the drag accelerations at a given altitude vary inversely with B, and the B-values of the Orbiter are already determined. (See Figures 4 and 5, reproduced from Reference 1. The quantity "BN" corresponds to B herein, except that the BN values specified in Reference 1 are expressed in lb/ft^2 rather than kg/m^2.)

Figure 3 provides the desired basic confirmation of feasibility, in that it shows the primary B^{-1} values* of the Orbiter in relation to values obtainable with a spherical free-flyer over a range of free-flyer mass (m) and average density (ρ) values. Figure 3 also indicates the along-orbit displacement rates Δs, in meters per revolution relative to an ideal drag-free satellite, which result at an altitude of 300 km. This information is conveniently provided on a second ordinate scale, a feature permitted by the dependence of Δs solely on B (per Appendix), for a given altitude and atmospheric density (U. S. Std. 1962, Reference 2, assumed here). Note that the desired relative displacement rates (free-flyer relative to Orbiter) can be read directly from Figure 3, as the difference between respective ordinate values, because of the linear relationship between Δs and B^{-1} (Equation 10, Appendix).

Results and Applications

As noted earlier, there are numerous possible modes of applying drag-induced maneuvers to the general separation and rendezvous problem. The basic requirement in all such applications is simply that the

*Use of the reciprocal ballistic coefficient B^{-1} is convenient here because of the direct variation of the orbital acceleration and displacement quantities with B^{-1}.

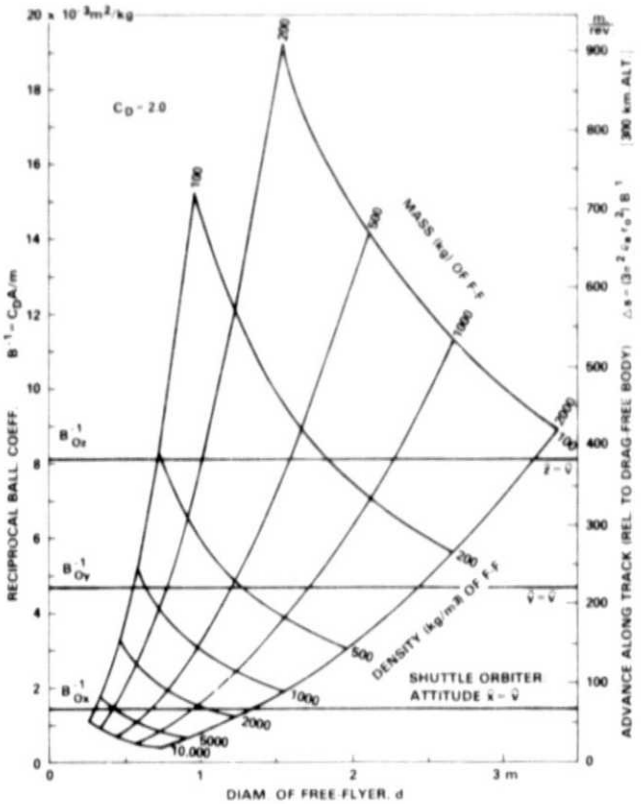

Fig. 3 Drag Effects on Spherical Free-Flyer Relative to Shuttle Orbiter

difference between the B^{-1} values of the Orbiter and the free-flyer be large enough and correctly directed to produce the desired relative motion.

If the Orbiter is to remain essentially passive (constant attitude and drag, no propulsion) throughout the separation and rendezvous mission, then the free-flyer must be capable of assuming B^{-1} values both above and below that of the Orbiter. There is no major difficulty in producing sufficiently large B^{-1} values in the free-flyer (e.g., the drag balloon described). The only substantial problem in free-flyer design arises in achieving B^{-1} values substantially below B^{-1}_{Ox} (Figure 3), which are required to obtain overtake of the free-flyer by the Orbiter in its minimum drag ($\hat{x} = \hat{v}$, or "head-on") attitude. This maneuver requires a free-flyer ballistic coefficient

Free-drift Orbiter mode

Estimates of the on-orbit acceleration levels, velocity increment makeup, and altitude decrease resulting from atmospheric drag on the Orbiter in a free-drift mode of operation are illustrated.* The drawing shows which axis of the spacecraft is perpendicular to orbit plane (POP) in the three attitude orientations. The ballistic numbers (BN's) are based on a 200,000-pound (90 718-kilogram) Orbiter having drag coefficient of 2.0.

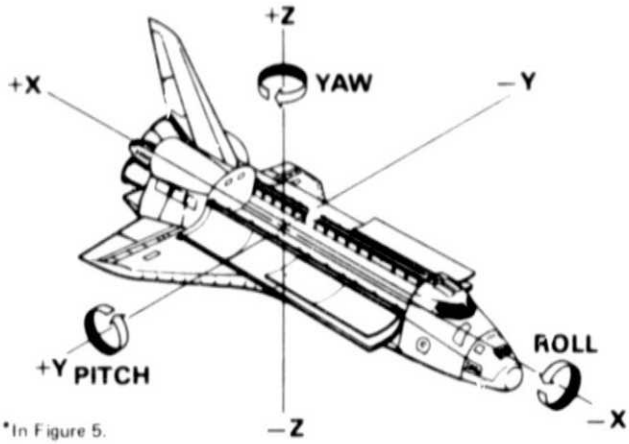

*In Figure 5.

Fig. 4 Shuttle Orbiter Reference Axes (Ref. 1)

in the "cannonball" range, $B^{-1} < 10^{-3}$ m²/kg, obtained by high densities and/or large sizes.** Since the free-flyer must be much smaller than the Orbiter, it must also be much more dense to achieve a lower B^{-1}.

A more tractable mission design is obtained when the Orbiter is in some other attitude, such as $\hat{y} = \hat{v}$ ("side-on"), as illustrated by Case No. 1 in the Table 1. After assuming the side-on attitude in Case No. 1, the performance parameters are chosen relatively freely: a 1-day forward separation motion of the free-flyer at moderate speed to a distance of 3 kilometers, followed by deliberately slower return over 4 days. These relative rates require, at 300 km altitude, free-flyer B^{-1} values of 8.7 and 3.7 x 10^{-3} m²/kg respectively, the

**The large size of the Orbiter contributes heavily to its relatively low $B^{-1}_{Ox} = 1.4 \times 10^{-3}$ m²/kg.

Table 1 Mission Characteristics -- Drag Separation and Rendezvous

Case No.	Orbiter Attitude	Free-Flyer Weight/Density	Maximum Separation	Flight Time (days) Separation	Rendezvous
1	$\hat{y} = \hat{v}$ (side-on)	500 kg (750 kg per m³)	3 km	1	4
2	$\hat{x} = \hat{v}$ (head-on)	1000 kg (4300 kg per m³)	3 km	1	8

latter entailing a moderate free-flyer density of 750 kg/m^3 under the 500 kg total mass assumption. The 1-day separation schedule implies a drag balloon of about 1.7 m. diameter.

Case No. 2 illustrates the design constraints imposed by the "worst case" cited above: the Orbiter overtaking in "head-on" attitude. In order to obtain free-flyer B^{-1} values appreciably below B_{Ox}^{-1} (Figure 3), the free-flyer mass is doubled relative to example 1, and its density is raised to a rather high 4300 kg/m^3. Even so, the closure rate is only half that of Case No. 1, so the rendezvous phase requires 8 days instead of 4. While these characteristics fall within practicable limits, they serve to illustrate the possible advantages of avoiding the head-on Orbiter overtake maneuver if overall operational considerations permit.

Overview

The above examples are given only to illustrate the range of performances and design latitude available under the simplest conditions, assuming a passive Orbiter. In practice, the Orbiter will not be completely passive, but rather will at least apply attitude control forces which are large compared to the drag forces considered here. Such applications will be brief, however, while the drag forces act continuously over periods of days, resulting in significant influences on the relative motion.

A rough quantitative comparison between the steady drag forces and the averaged attitude control forces can be obtained by comparing the drag makeup velocity increment values in Figure 5 (taker from Reference 1) to the typical vernier jet propellant usage estimates given

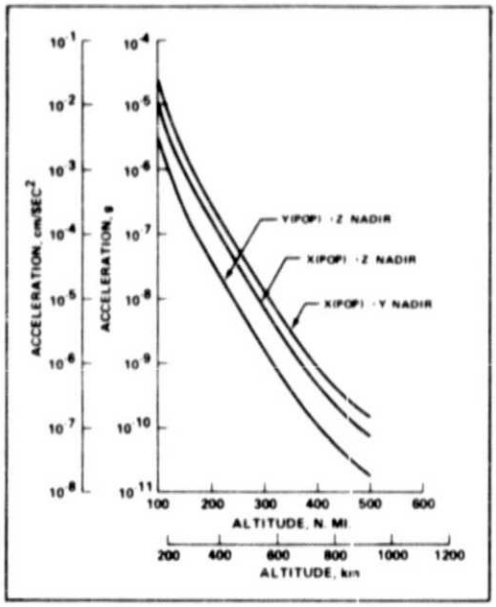

Effects of atmospheric drag on the Orbiter.

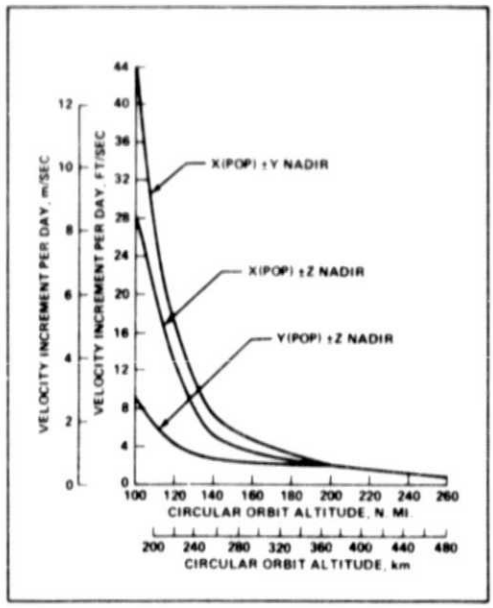

Drag makeup delta-V increment in circular orbit.

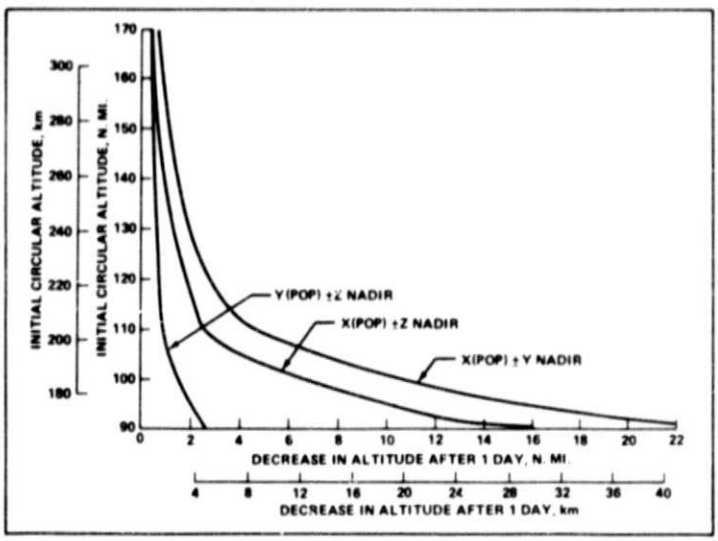

Effects of drag on the Orbiter in low-Earth circular orbit.

Fig. 5 Drag Effects on Shuttle Orbiter in Three Orthogonal Attitudes as Function of Altitude (Ref. 1)

in Reference 4 (Table 3.4). Figure 5 indicates a drag makeup Δv of about 0.7 m/sec per day for an Orbiter at 300 km altitude in the X $\perp$ V attitude (Y-POP $\pm$ Z nadir in the Reference designations), whereas a total Δv of about 0.2 m/sec per day results from attitude control impulses via the Reference 4 data ($\sim$ 0.3 kg/hr propellant at 228 sec specific impulse). More importantly, the attitude control impulses will not be cumulative like the drag effects, but will act in various directions and add vectorially to a resultant probably close to zero.

It is clear also that some propulsive maneuvering by the Orbiter will be required in practice to make corrections and control the final approach and capture operation. The present objective is simply to show that a significant portion of the overall separation and capture mission can be accomplished inexpensively by harnessing the available drag forces.

References

1. Space Transportation System User Handbook, NASA, Washington, D.C. 20546, June 1977.

2. U.S. Standard Atmosphere, 1962, U.S. Government Printing Office, Washington, D.C. 20402, December 1962.

3. U.S. Standard Atmosphere, 1976, U.S. Government Printing Office, Washington, D.C. 20402, October 1976.

4. Space Shuttle System Payload Accommodations, JSC-07700 Volume XIV, Lyndon B. Johnson Space Center, Houston, Texas 77058, June 17, 1977.

Appendix
Drag Effects on Nearly Circular Satellite Motion -- An Analytical Approximation

Drag-Free Motion

The idealized Keplerian motion (inverse square gravity, no drag or other perturbations) of a small body in a circular satellite orbit is specified by a constant radial distance (r_o) and a constant angular velocity ($\dot{\theta}$) obeying Kepler's Third Law:

$$r = r_o$$
$$\theta = \dot{\theta} t = 2\pi t/\tau = \sqrt{K/r_o^3}\ t \qquad (1)$$

where $\tau = 2\pi\sqrt{r_o^3/K}$, the orbital period

and $K = GM_\oplus$, the earth gravitational parameter ($K = 3.986 \times 10^{14}\ m^3/sec^2$)

In the absence of drag or other perturbing influences, this idealized circular motion continues indefinitely without change.

The Drag Force

It is not realistic, however, to neglect drag forces over appreciable time intervals, especially for satellites at relatively low altitudes. Hence we seek a convenient way of modifying the above relationships to account for the drag force F_D, expressed in its fundamental form as

$$F_D = \tfrac{1}{2} C_D A \rho_a v^2 \qquad (2)$$

where C_D is the drag coefficient

A is the characteristic frontal area of the body

ρ_a is the atmospheric density at $r = r_o$

v is the velocity of the body in its circular orbit at $r = r_o$ ($v = \sqrt{K/r_o}$)

Energy and Altitude Losses to Drag

Because the Keplerian motion is energy conservative and the drag effect is conveniently expressed as an energy loss rate, it is logical to relate the two through the conservation of energy principle. Specifically, the drag work done on the body (dW), or its energy change dE, over an infinitesimal displacement ds is simply $dE = F_D\, ds$, since the drag force is parallel to the flight path. Dividing that expression by dt, we have the energy loss rate due to drag

$$\dot{E} = F_D \dot{s} = F_D v = \tfrac{1}{2} C_D A \rho_a v^3 \qquad (3)$$

Energy conservation requires that this energy loss be extracted from the orbital energy of the satellite, which is

$$\begin{aligned} E &= T + V \\ &= m\left[(v^2/2 - (K/r)\right] \\ &= -mK/2r_o \end{aligned} \qquad (4)$$

since $v^2 = K/r_o$ for circular orbits.

The orbital energy loss to drag appears as a steadily decreasing orbital radius:

$$\dot{E} = -(mK/2r_o^2)\ \dot{r}$$
$$\dot{r} = -(2r_o^2/mK)\ (\tfrac{1}{2} C_D A\ \rho_a v_o^3)$$
$$\dot{r} = -B^{-1}\ \rho_a r_o^2 v_o^3/K$$

where $B^{-1} = C_D A/m$, the reciprocal of the ballistic coefficient $B = m/C_D A$.

Since $r_o v_o^2 = K$, the above expression for $\dot{r}$ becomes

$$\dot{r} = -B^{-1}\ \rho_a r_o v_o \qquad (5)$$

The altitude decay Δh per revolution is (approximately) the above decay rate times the orbit period at the initial altitude:

$$\begin{aligned} \Delta h = \dot{r}\tau_o &= (2\pi r_o/v_o)\ (-B^{-1}\ \rho_a r_o v_o) \\ &= -2\pi B^{-1}\ \rho_a r_o^2 \end{aligned} \qquad (6)$$

Angular Acceleration and Displacement

Because the decreasing altitude involves a correspondingly decreasing period, the orbital angular velocity $\dot{\theta}$ increases steadily, which causes the drag-affected satellite to move ahead of a reference drag-free satel-

lite (constant $\dot{\theta}$) in orbital position θ. The drag-induced angular acceleration ($\ddot{\theta}$) specifying this effect is obtained by rearranging the basic expression for orbit period (Equation 1) and differentiating:

$$\ddot{\theta} = (d/dt)\sqrt{K/r_o^3} = -(3/2)\sqrt{K/r_o^5}\,\dot{r} \qquad (7)$$

Substituting Equation (5) into Equation (7) and noting that $v_o = \sqrt{K/r_o}$,

$$\ddot{\theta} = -(3/2)\sqrt{K/r_o^5}\,(-B^{-1}\rho_a r_o\sqrt{K/r_o}) = 3B^{-1}\rho_a K^{1/2} r_o^{1/2} \qquad (8)$$

The drag-induced advance in position angle $\Delta\theta$ per revolution takes the familiar form

$$\Delta\theta = \ddot{\theta}\pi r_o^2/2 = (3B^{-1}\rho_a K^{1/2} r_o^{1/2})4\pi^2 r_o^3/K = 3\pi^2 B^{-1}\rho_a r \qquad (9)$$

The corresponding linear circumferential advance along the orbit Δs per revolution follows directly:

$$\Delta s = r_o \Delta\theta = 3\pi^2 B^{-1}\rho_a r_o^2 \qquad (10)$$

Numerical Results

The variations of Δh and Δs per revolution with altitude and reciprocal ballistic coefficient are shown in Figure 6. The curves are based on calculations using Equations (6) and (10), together with mean values of the atmospheric density ρ_a obtained from the U. S. Standard Atmosphere, 1976 (Reference 3). These density values are also plotted separately in Figure 6, along with the corresponding U. S. Standard Atmosphere, 1962 (Reference 2) curve provided for comparison.

It is important to understand that the actual density curve at a given time may vary widely from the mean, by a factor of two or more, primarily in response to variations in solar activity. Comparable wide variations in Δh and Δs must be expected also, since they vary linearly with the actual density ρ_a.

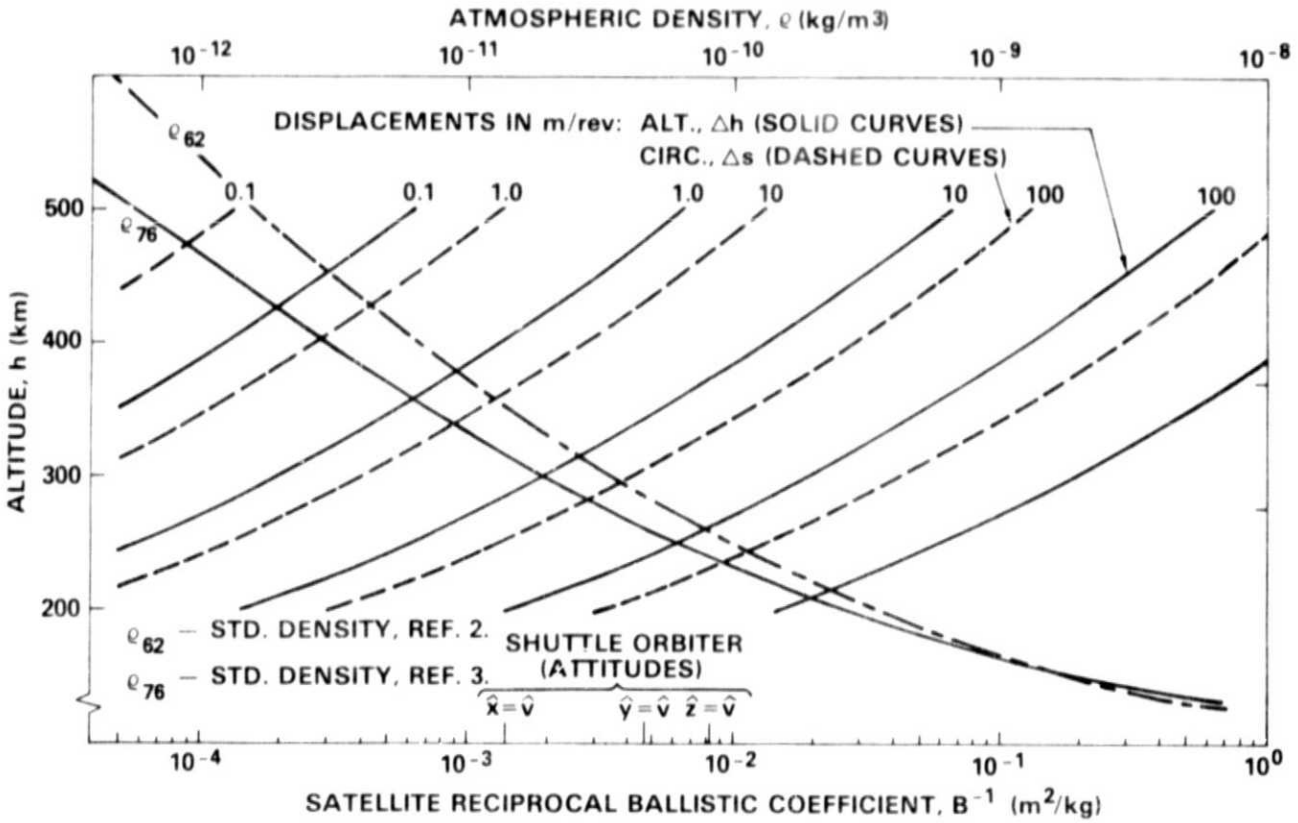

Fig. 6 Drag Perturbations of Satellites in Circular Orbits